Pressure Swing Adsorption

Part III: Numerical Simulation of a Kinetically Controlled Bulk Gas Separation

A numerical simulation has been developed for a simple two-bed PSA system in which kinetic effects and changes in flow rate due to adsorption are significant. The model is therefore more general than most previous models for the PSA cycle. The model equations are solved by the method of double collocation. When applied to air separation on a carbon molecular sieve, using independently measured kinetic and equilibrium parameters, the predicted performance appears consistent with available performance data for a commercial unit.

N. S. RAGHAVAN and D. M. RUTHVEN

Department of Chemical Engineering
University of New Brunswick
Fredericton, N.B., Canada

SCOPE

In many PSA separation processes (e.g., air separation on a carbon molecular sieve) kinetic effects are important and the volume of gas adsorbed is significant. Under these circumstances the assumptions which have been traditionally employed in modeling of the PSA cycle (adsorption equilibrium, constant velocity) are no longer valid. In the present analysis a more general mathematical model for simulation of a PSA cycle is developed without recourse to either of these simplifying assumptions. This model, which should be directly applicable to air separation as well as to other bulk PSA separations, is solved numerically by the method of double collocation using parameter values typical of air separation on a carbon molecular sieve.

CONCLUSIONS AND SIGNIFICANCE

The model appears to provide a reasonable representation of the behavior of a two-bed PSA adsorption system. Using independently measured kinetic and equilibrium parameters the predicted performance is comparable with the reported performance of the commercial units, suggesting that the basic assumptions as well as the approximations used to represent the blowdown and repressurization steps are reasonable. The method of double collocation is shown to be a useful tool for solving complicated model equations for such systems, and the approach delineated here seems capable of being extended to the simulation of the more complicated PSA cycles commonly used in commercial processes. Although in the present analysis the equilibrium relationships are assumed to be linear, such an assumption is not critical and the same general method may be applied to a nonlinear system without any significant increase in complexity. Although the analysis has been developed in relation to air separation on a carbon molecular sieve, the simulation is in principle applicable to other PSA bulk separations where kinetic effects and volume changes are significant.

INTRODUCTION

Efficient performance of a pressure swing adsorption (PSA) unit depends on achieving the correct combination of process variables such as bed length, flow rate, cycle time, pressure ratio, and purge to feed ratio. The effects of these variables are coupled so that it is difficult to arrive at an optimal design simply by intuition and empiricism; a reliable mathematical simulation of the system is therefore required. Because of the transient nature of the process and the complexity of the equations describing the system dynamics, it has not hitherto been possible to obtain a general mathematical simulation. Various *simplifying assump-*

N. S. Raghavan is currently with Alcan International Ltd., Kingston, Ontario, Canada.

tions have therefore been introduced. If mass transfer is sufficiently rapid one may neglect mass transfer resistance and assume that equilibrium is always maintained. This approach, which has been developed by Turnock and Kadlec (1971) and by Hill and coworkers (Chan et al., 1981; Knaebel and Hill, 1982), has proved useful in defining the qualitative effects of the process variables and the region within which acceptable operating conditions must lie.

For air separation on a zeolite adsorbent the validity of the equilibrium approximation under conditions typical of a PSA cycle has been verified by Florez-Fernandez and Kenney (1983). However, the equilibrium approximation is certainly not universally valid; in particular, it is invalid for air separation on a carbon molecular sieve, which depends on kinetic selectivity rather than on differences in adsorption equilibrium between oxygen and nitrogen.

Simulations in which kinetic effects were included have been presented by Shendalman and Mitchell (1972), Mitchell and Shendalman (1973), Raghavan et al. (1985), and Chihara and Suzuki (1983), who also included the heat balance. In all these simulations it was assumed that the adsorbable species is present only at trace concentrations in an inert carrier. This approximation, which is generally appropriate for hydrogen purification systems and "heatless driers," simplifies considerably the mathematical problems involved in the simulation since changes in flow rate due to adsorption can be neglected. However, for air separation such an approximation is clearly inappropriate. In the present paper we summarize the development and solution of a more general PSA model which includes kinetic effects and allows also for the variation in flow rate due to adsorption. Although developed with particular reference to air separation on a carbon molecular sieve, this model is in fact applicable more generally to any separation in which kinetic effects and volume changes are significant.

MATHEMATICAL MODEL

The basic PSA cycle involves four distinct steps, as shown in Figure 1. During step 1 a high-pressure feed (in our case air) is supplied continuously to bed 2, which is packed with carbon molecular sieve (CMS) pellets in which oxygen is adsorbed more rapidly than nitrogen. The nitrogen, which remains in the gas phase, passes through the bed and is removed as pure raffinate product. A small fraction of this stream is expanded to low pressure and used to purge bed 1 (which is also packed with CMS pellets). In step 2, bed 1 is pressurized with feed while bed 2 is subjected to a pressure reduction (blowdown). The same cycle is repeated in steps 3 and 4 with high-pressure flow and adsorption occurring in bed 1 and purging occurring in bed 2. In order to develop a mathematical model the following approximations are introduced:

1. The system is considered isothermal with total pressure remaining constant throughout the bed during high-pressure and low-pressure flow operations (steps 1 and 3).
2. The flow pattern is described by the axial dispersed plug flow model.
3. The equilibrium relationships for both oxygen and nitrogen are assumed linear.
4. Mass transfer rates are represented by linear driving force expressions and the rate coefficient is the same for both high-pressure and low-pressure steps. This is a reasonable assumption for a system in which micropore diffusion is the dominant mass transfer resistance.

The additional approximations which are needed in order to simplify the mathematical description of the blowdown and repressurization steps are discussed below.

Subject to these assumptions, the dynamic behavior of the system may be described by the following set of equations ($A = O_2$; $B = N_2$):

Step 1. High-Pressure Flow in Bed 2 and Low-Pressure (Purge) Flow in Bed 1

External fluid phase in bed 2:

$$\frac{\partial C_{A2}}{\partial t} - D_{L2}\frac{\partial^2 C_{A2}}{\partial z^2} + v_2\frac{\partial C_{A2}}{\partial z} + C_{A2}\frac{\partial v_2}{\partial z} + \left(\frac{1-\epsilon}{\epsilon}\right)\frac{\partial q_{A2}}{\partial t} = 0 \tag{1}$$

$$\frac{\partial C_{B2}}{\partial t} - D_{L2}\frac{\partial^2 C_{B2}}{\partial z^2} + v_2\frac{\partial C_{B2}}{\partial z} + C_{B2}\frac{\partial v_2}{\partial z} + \left(\frac{1-\epsilon}{\epsilon}\right)\frac{\partial q_{B2}}{\partial t} = 0 \tag{2}$$

$$C_{A2} + C_{B2} = C_{HP}\ (\text{constant}) \tag{3}$$

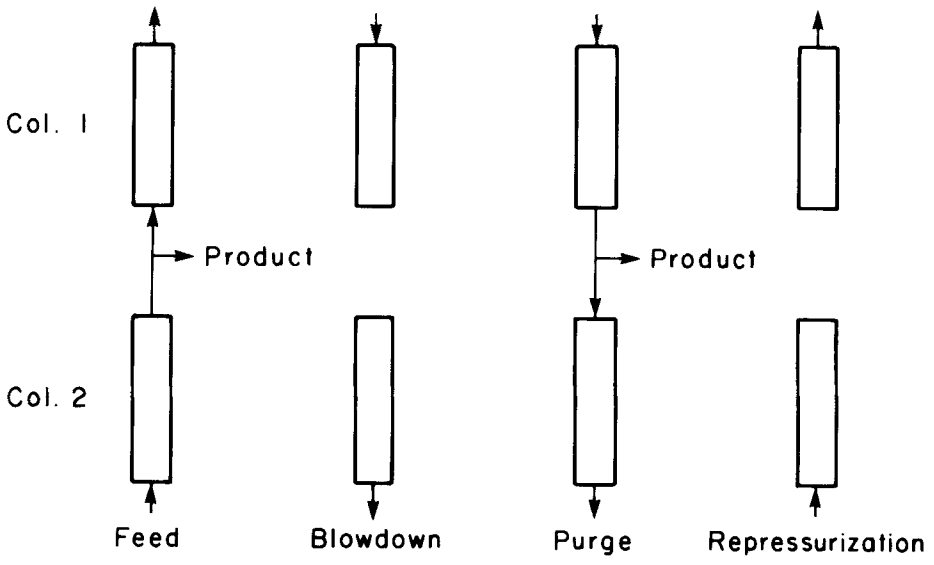

Figure 1. Steps involved in a PSA cycle.

Adding Eqs. 1 and 2, and considering Eq. 3,

$$C_{HP}\frac{\partial v_2}{\partial z}+\left(\frac{1-\epsilon}{\epsilon}\right)\frac{\partial q_{A2}}{\partial t}+\left(\frac{1-\epsilon}{\epsilon}\right)\frac{\partial q_{B2}}{\partial t}=0 \tag{4}$$

Solid phase in bed 2:

$$\frac{\partial q_{A2}}{\partial t}=k_A\,(q^*_{A2}-q_{A2}) \tag{5}$$

$$\frac{\partial q_{B2}}{\partial t}=k_B\,(q^*_{B2}-q_{B2}) \tag{6}$$

where:

$$q^*_{A2}=K_AC_{A2};\quad q^*_{B2}=K_BC_{B2} \tag{7}$$

Boundary conditions:

$$D_{L2}\left.\frac{\partial C_{A2}}{\partial z}\right|_{z=0}=-v_{OH}(C_{A2}|_{z=0^-}-C_{A2}|_{z=0^+}) \tag{8}$$

$$\left.\frac{\partial C_{A2}}{\partial z}\right|_{z=L}=0 \tag{9}$$

External fluid phase in bed 1:

$$\frac{\partial C_{A1}}{\partial t}-D_{L1}\frac{\partial^2 C_{A1}}{dz^2}+v_1\frac{\partial C_{A1}}{\partial z}+C_{A1}\frac{\partial v_1}{\partial z}+\left(\frac{1-\epsilon}{\epsilon}\right)\frac{\partial q_{A1}}{\partial t}=0 \tag{10}$$

$$\frac{\partial C_{B1}}{\partial t}-D_{L1}\frac{\partial^2 C_{B1}}{\partial z^2}+v_1\frac{\partial C_{B1}}{\partial z}+C_{B1}\frac{\partial v_1}{\partial z}+\left(\frac{1-\epsilon}{\epsilon}\right)\frac{\partial q_{B1}}{\partial t}=0 \tag{11}$$

$$C_{A1}+C_{B1}=C_{LP}\ (\text{constant}) \tag{12}$$

Adding Eqs. 10 and 11, and considering Eq. 12,

$$C_{LP}\frac{\partial v_1}{\partial z}+\left(\frac{1-\epsilon}{\epsilon}\right)\frac{\partial q_{A1}}{\partial t}+\left(\frac{1-\epsilon}{\epsilon}\right)\frac{\partial q_{B1}}{\partial t}=0 \tag{13}$$

Solid phase in bed 1:

$$\frac{\partial q_{A1}}{\partial t}=k_A\,(q^*_{A1}-q_{A1}) \tag{14}$$

$$\frac{\partial q_{B1}}{\partial t}=k_B\,(q^*_{B1}-q_{B1}) \tag{15}$$

where:

$$q^*_{A1}=K_AC_{A1};\quad q^*_{B1}=K_BC_{B1} \tag{16}$$

Boundary conditions:

$$D_{L1}\left.\frac{\partial C_{A1}}{\partial z}\right|_{z=0}=-v_{OL}(C_{A1}|_{z=0^-}-C_{A1}|_{z=0^+}) \tag{17}$$

where:

$$C_{A1}|_{z=0^-}=C_{A2}|_{z=L,\,P=P_L} \tag{18}$$

$$\left.\frac{\partial C_{A1}}{\partial z}\right|_{z=L}=0 \tag{19}$$

The initial conditions for the start-up of the cyclic operation with two clean beds are the following two sets of equations:

$$\begin{aligned} &C_{A2}(z,\,t=0)=0;\quad C_{B2}(z,\,t=0)=0;\\ &q_{A2}(z,\,t=0)=0;\quad q_{B2}(z,\,t=0)=0\\ &C_{A1}(z,\,t=0)=0;\quad C_{B1}(z,\,t=0)=0;\\ &q_{A1}(z,\,t=0)=0;\quad q_{B1}(z,\,t=0)=0 \end{aligned} \tag{20}$$

Since C_{B2} can be found from C_{HP} and C_{A2} (for high-pressure flow in bed 2), and C_{B1} can be found from C_{LP} and C_{A1} (for low-pressure flow in bed 1), the equations which have been solved simultaneously along with the relevant boundry conditions are Eqs. 1, 4, 5, 6, 10, 13, 14, and 15.

Step 2. Blowdown of Bed 2 and Pressurization of Bed 1

For blowdown, the following two approximations are introduced:

TABLE 1. EXIT COMPOSITION OF OXYGEN, AND EXIT FLUID VELOCITY IN BED 2 AT END OF STEP 1 OF STEADY-STATE PSA OPERATION ASSUMING SOLID PHASE CONCENTRATIONS OF O_2 AND N_2 FROZEN DURING BLOWDOWN*

Effect of	Parameter Values: α s	G	t_{max} s	k_A s^{-1}	k_B s^{-1}	K_A	K_B	P_{eH}	P_{eL}	Exit compos. of O_2 X_{A2}	Exit fluid velocity V_2
Bed length to feed inlet velocity ratio, α	20	2	60	0.040	0.0016	9.35	9.35	∞	∞	0.0148	0.667
	30	2	60	0.040	0.0016	9.35	9.35	∞	∞	0.0076	0.560
	40	2	60	0.040	0.0016	9.35	9.35	∞	∞	0.0032	0.470
Purge to feed velocity ratio, G	30	1	60	0.040	0.0016	9.35	9.35	∞	∞	0.0266	0.575
	30	2	60	0.040	0.0016	9.35	9.35	∞	∞	0.0076	0.560
	30	3	60	0.040	0.0016	9.35	9.35	∞	∞	0.0024	0.550
Time duration for adsorption/desorption (step 1 or 3), t_{max}	30	2	30	0.040	0.0016	9.35	9.35	∞	∞	0.0150	0.475
	30	2	60	0.040	0.0016	9.35	9.35	∞	∞	0.0076	0.560
	30	2	90	0.040	0.0016	9.35	9.35	∞	∞	0.0063	0.615
	30	2	120	0.040	0.0016	9.35	9.35	∞	∞	0.0061	0.633
	30	2	180	0.040	0.0016	9.35	9.35	∞	∞	0.0063	0.657
	30	2	240	0.040	0.0016	9.35	9.35	∞	∞	0.0110	0.670
Axial dispersion, P_{eH}, P_{eL}	30	2	60	0.040	0.0016	9.35	9.35	100	100	0.0092	0.562
	30	2	60	0.040	0.0016	9.35	9.35	10	10	0.0273	0.572
Overall mass transfer coefficients, k_A and k_B	30	2	60	0.0026**	0.000106**	9.35	9.35	∞	∞	0.1580	0.902

* Bed porosity, $\epsilon = 0.40$; Temp. of PSA operation = 298 K; P_L = 1 atm (101.3 kPa); P_H = 3 atm (303.9 kPa); $k_A = 15\,D_A/r^2$; $k_B = 15\,D_B/r^2$.
** Values for D_A/r^2 and D_B/r^2 reported by Knoblauch (1978).

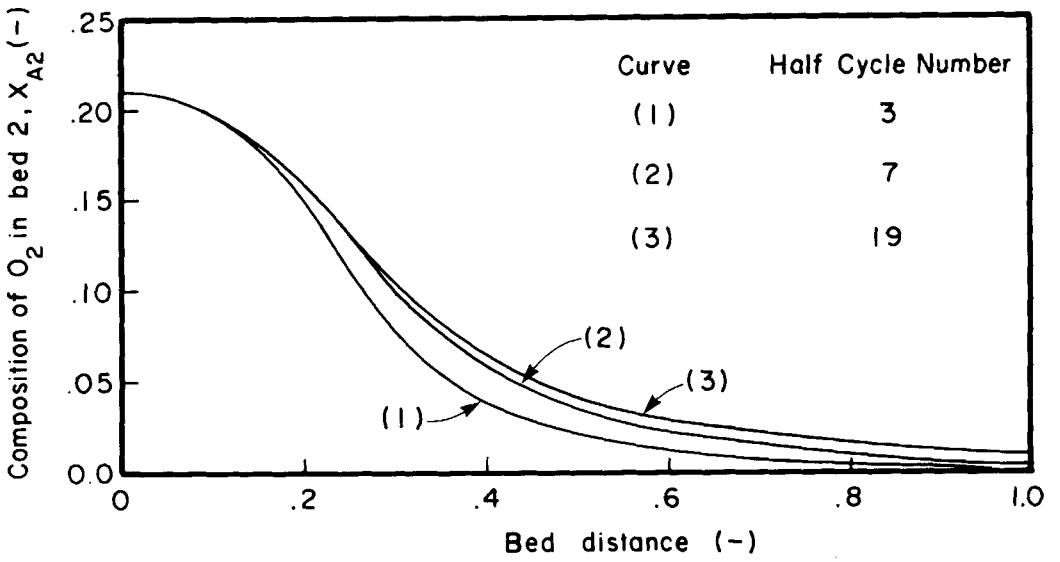

Figure 2. Gas phase composition profiles of oxygen in bed 2 at end of high-pressure (adsorption) step, showing progress toward cyclic steady state. Parameter values as for ratio *G* (row 2, Table 1).

1. The gas phase concentrations of O_2 and N_2 at the end of blowdown correspond to the concentrations at each and every position in the bed at the end of the preceding high-pressure flow adsorption step multiplied by the pressure ratio, P_L/P_H, where P_H is the pressure at which adsorption is carried out and P_L is the purge or desorption pressure.

2. In one version of the simulation the solid phase concentrations of O_2 and N_2 are assumed to remain frozen. The results presented in Table 1 and Figures 2–6 are based on this assumption for the solid phase concentrations during blowdown. However, a number of simulations were also performed in which the oxygen in the adsorbed phase was assumed to reach equilibrium at the low pressure:

$$q_{A2} = K_A C_{A2}|_{P_L} \tag{21}$$

The slower diffusing nitrogen was assumed to remain frozen. The results presented in Table 2 are based on these assumptions.

For pressurization of bed 1, the following two approximations are introduced:

1. During pressurization by feed air, the fluid phase O_2 and N_2 remaining in the bed from the preceding low-pressure purge flow operation are pushed in plug flow toward the closed end of the bed through a distance given by $(1 - P_L/P_H)$ from the feed inlet. Thus for example, if the pressure ratio, P_L/P_H is 0.33, then the concentrations of O_2 and N_2 at the end of pressurization are the average of the respective concentrations that existed through the entire length of the bed at the end of the preceding low-pressure purge flow. However, these average concentrations exist only through a dimensionless length of 0.33 from the closed end of the bed, the remainder being filled with the pressurizing feed

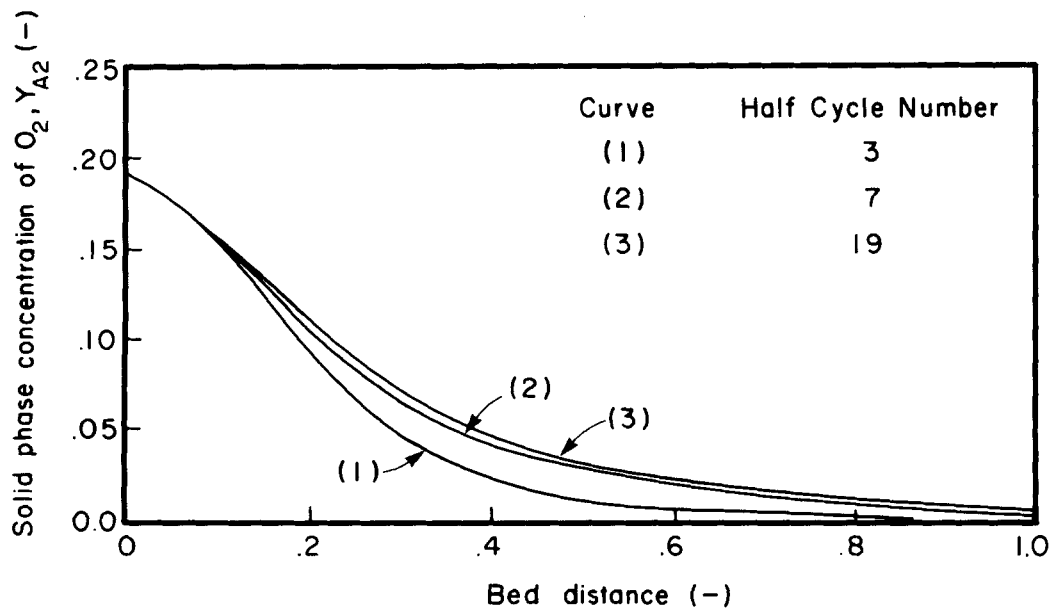

Figure 3. Solid phase concentration profiles of oxygen in bed 2 at the end of high-pressure (adsorption) step, showing progress toward cyclic steady state. Parameter values as for ratio *G* (row 2, Table 1).

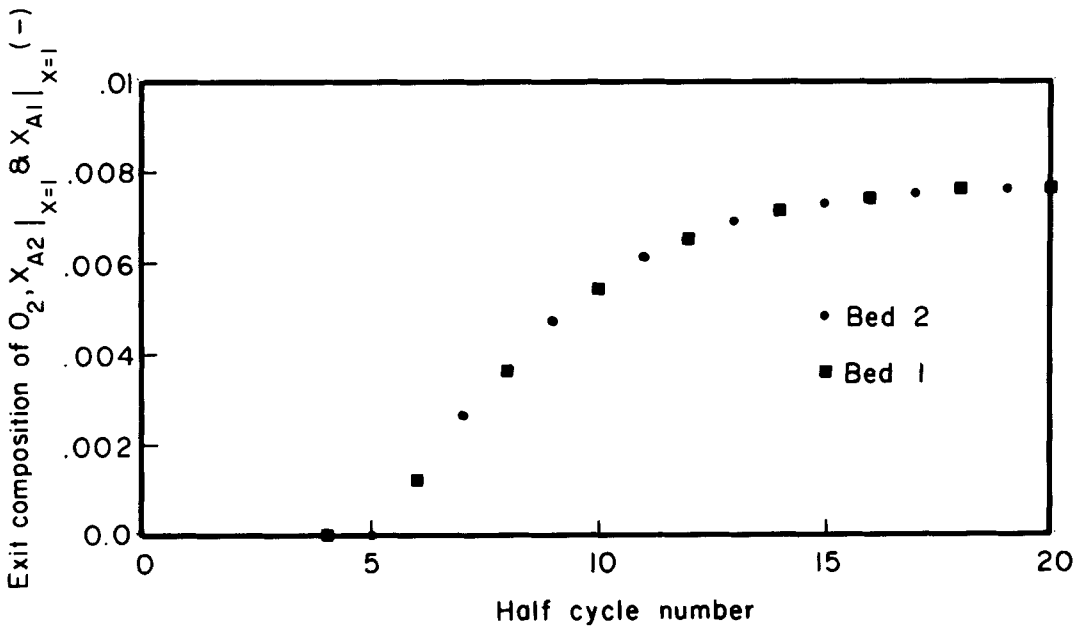

Figure 4. Exit gas phase composition of oxygen at end of high-pressure (adsorption) step as a function of half-cycle number. Parameter values as for ratio *G* (row 2, Table 1).

air. While this is obviously a somewhat crude approximation it is clearly more realistic than assuming a uniform composition in the gas phase.

2. The solid phase concentrations of O_2 and N_2 remain unchanged at the values of the end of the preceding low pressure purge flow. This assumption is physically reasonable since the pressurization is very rapid compared to $r^2/15\,D$ for O_2 and N_2 in the present study.

Step 3

This step is virtually the same as step 1, except that here the high-pressure feed flows through bed 1 while a portion of the exit product (N_2) purges bed 2 at the low operating pressure. The equations which have been solved to describe this step are identical to those solved for step 1, but with the change in the direction of flow taken into account.

Step 4

The approximations made for step 2 are valid for step 4, the difference being that bed 1 is now subjected to pressure reduction (blowdown) and bed 2 is pressurized.

The above equations were written in dimensionless form and solved to give the O_2 composition, C_{A2}/C_{HP}, C_{A1}/C_{LP} (step 1), C_{A2}/C_{LP}, C_{A1}/C_{HP} (step 3) in the fluid phase, and O_2 and N_2 concentrations, q_{A2}/K_AC_{HP}, q_{B2}/K_BC_{HP}, q_{A1}/K_AC_{HP}, q_{B1}/K_BC_{HP}, (steps 1 and 3) in the solid phase, as functions of dimensionless bed distance (z/L) at various times (τ). The final cyclic steady-state profiles were determined by continuing the

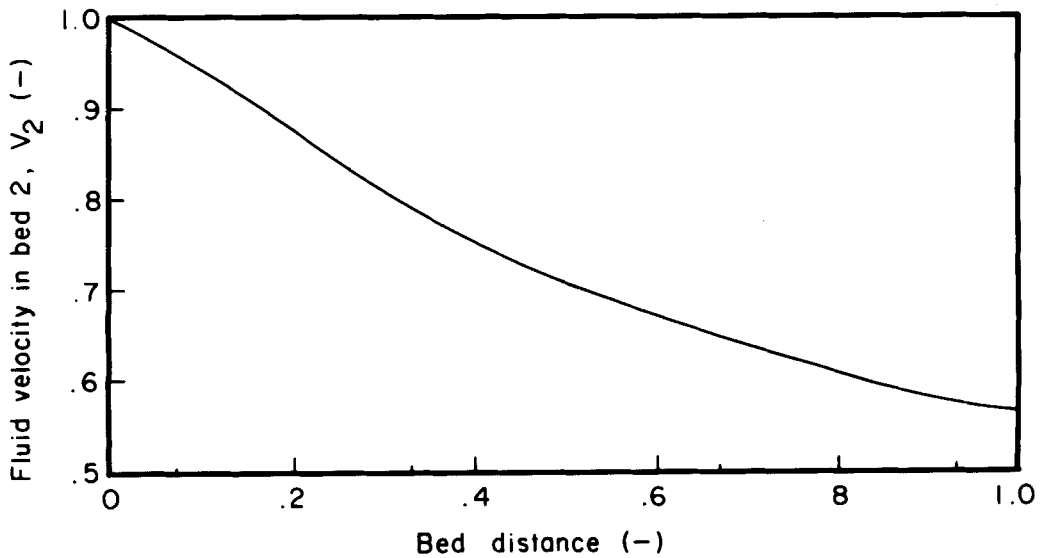

Figure 5. Fluid velocity as a function of distance in bed 2 at end of high-pressure (absorption) step at cyclic steady states. Parameter values as for ratio *G* (row 2, Table 1).

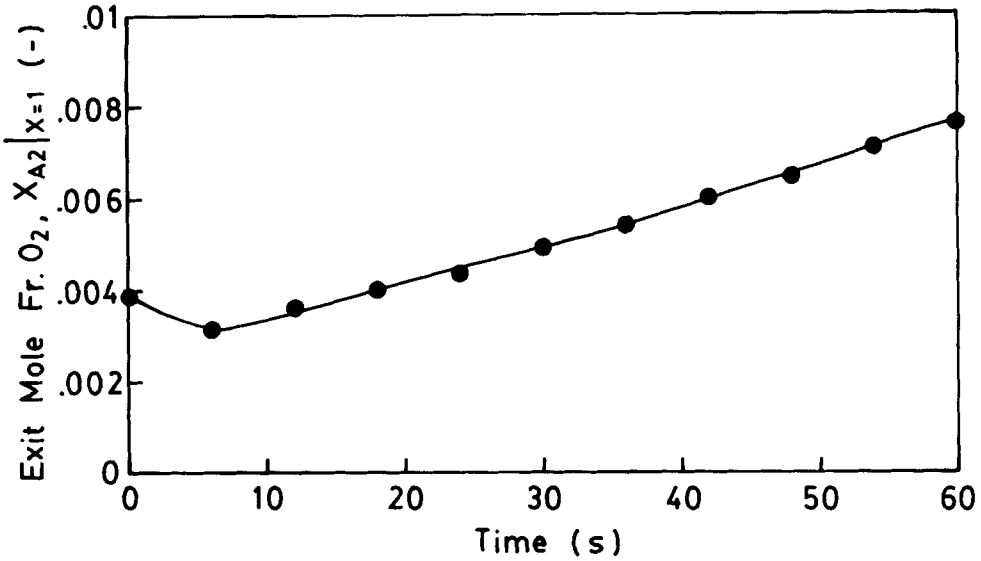

Figure 6. Exit gas phase mole fraction of oxygen during high-pressure (adsorption) step at cyclic steady state as a function of time. Parameter values as for ratio *G* (row 2, Table 1).

simulation for sufficient cycles until no significant further changes in the profile occurred. By repeating the simulation with different sets of parameters the effects of the purge/feed ratio ($G = v_{OL}/v_{OH}$), the bed length/inlet feed velocity ($\alpha = L/v_{OH}$), the time duration (t_{max}) of the adsorption and desorption steps and the axial Peclet number ($Pe = v_{OH}L/D_L$) were studied.

METHOD OF SOLUTION

In our earlier paper on PSA simulation(Raghavan et al. 1985), in which we considered adsorption of a single trace component without velocity variation, we solved the relevant partial differential equations by reducing them to sets of ordinary differential equations by the method of orthogonal collocation. However, application of the same procedure to the solution of Eqs. 1, 4, 5, and 6 (for bed 2, step 1) or Eqs. 10, 13, 14, and 15 (for bed 1, step 1) would lead to sets of ordinary differential equations (Eqs. 1, 5, 6, 10, 14, and 15) together with sets of nonlinear algebraic equations (Eqs. 4 and 13). Such a combination of ordinary differential and nonlinear algebraic equations is likely to cause stiffness and convergence problems. Therefore, the method of double collocation was applied so that all the equations would be reduced to sets of algebraic equations (Young and Finlayson, 1973). Details of the method are given in the appendix.

RESULTS AND DISCUSSION

In order to test the validity of the model, values of the diffusional time constants and equilibrium constants for oxygen and nitrogen are required. The equilibrium constants were obtained directly from the isotherms given by Knoblauch (1978). Limited kinetic data are also presented in this article suggesting that the ratio of diffusivities (D_A/D_B) is about 25 ($D_A/r^2 = 1.7 \times 10^{-4}$ s^{-1}, $D_B/r^2 \approx 7 \times 10^{-6}$ s^{-1}). Using these values it was found that the concentration of oxygen in the nitrogen product was always unreasonably high (10–15%), whereas in practice the oxygen concentration can be reduced to less than 1%. A limited experimental study of the sorption kinetics of O_2 and N_2 in Bergbau-Forschung carbon sieve was therefore undertaken by both chromatographic and gravimetric methods. This revealed that the ratio of diffusivities is indeed about 25 but the actual values of D/r^2 are much higher ($D_a/r^2 \approx 2.66 \times 10^{-3}$ s^{-1}; $D_B/r^2 \approx 1.06 \times 10^{-4}$ s^{-1}). Using the linear driving force representation ($k = 15(D/r^2)$) we obtain $k_A = 0.04$ s^{-1}, $k_B = 0.0016$ s^{-1}.

The parameter values and the results from the numerical simulation are summarized in Tables 1 and 2. All simulations were performed with the assumption of an initially clean bed. Some of the results that could not be presented in a tabular form are shown in Figures 2–6.

The progress toward the cyclic steady state profile is shown in Figure 2. Under the conditions of this simulation the final steady-state nitrogen composition in the product is about 99.2%. Figure 3 contains curves showing the solid phase concentration of oxygen as a function of bed distance for various half-cycle numbers (for our purposes of simulation, one half-cycle will comprise either steps 1 and 2 or steps 3 and 4, with the first half-cycle ending when step 2 is completed) until cyclic steady state is reached. In Figure 4 the compositions of oxygen at the outlet of the two beds when they are subjected to high-pressure adsorption are presented as a function of the half-cycle number. It is seen that the two beds essentially lead to the same extent of product purity on their approach toward the cyclic steady state. The variation of gas velocity through the bed at the end of the high pressure adsorption step is shown in Figure 5. It is clear that for this system the assumption of a uniform gas velocity would be a poor approximation. Figure 6 shows the exit composition of oxygen in bed 2 as a function of time during the adsorption step at cyclic steady state. It is evident that at the start of this step the oxygen composition falls from a higher value to a lower value. This drop is then followed by an increase in the oxygen concentration. This behavior is understandable since the adsorption step is preceded by the repressurization of the bed, during which the residual oxygen is pushed toward the bed outlet. We therefore see an initial high level of oxygen at the outlet at the start of the high-pressure adsorption step.

As may be seen from Tables 1 and 2, the effects of bed length/inlet velocity, and purge/feed velocity on the concentration of oxygen in the product show the expected trends; i.e., with an increase in L/v_{OH} and G the nitrogen purity improves. However, with either assumption for solid phase concentration of oxygen during blowdown (frozen as for simulations under item 3 in Table 1 or as given by Eq. 21, item 3, Table 2), the oxygen composition exhibits a minimum as the time for steps 1 and 3 is increased. This indicates that for the conditions such as bed

TABLE 2. EXIT COMPOSITION OF OXYGEN, AND EXIT FLUID VELOCITY IN BED 2 AT END OF STEP 1 OF STEADY-STATE PSA OPERATION BASED ON BLOWDOWN EQUILIBRIUM ASSUMPTION FOR O_2 (EQ. 21)*

Effect of	Parameter Values									Exit compos. of O_2	Exit fluid velocity
	α s	G	t_{max} s	k_A s^{-1}	k_B s^{-1}	K_A	K_B	P_{eH}	P_{eL}	X_{A2}	V_2
Bed length to feed inlet velocity ratio, α	20	2	60	0.040	0.0016	9.35	9.35	∞	∞	0.0047	0.647
	30	2	60	0.040	0.0016	9.35	9.35	∞	∞	0.0012	0.555
	40	2	60	0.040	0.0016	9.35	9.35	∞	∞	0.0000	0.465
Purge to feed velocity ratio, G	30	1	60	0.040	0.0016	9.35	9.35	∞	∞	0.0036	0.557
	30	2	60	0.040	0.0016	9.35	9.35	∞	∞	0.0012	0.555
	30	3	60	0.040	0.0016	9.35	9.35	∞	∞	0.0001	0.555
Time duration for adsorption/desorption (step 1 or 3), t_{max}	30	2	18	0.040	0.0016	9.35	9.35	∞	∞	0.0018	0.421
	30	2	30	0.040	0.0016	9.35	9.35	∞	∞	0.0009	0.490
	30	2	60	0.040	0.0016	9.35	9.35	∞	∞	0.0012	0.555
	30	2	90	0.040	0.0016	9.35	9.35	∞	∞	0.0024	0.613
Axial dispersion, P_{eH}, P_{eL}	30	2	60	0.040	0.0016	9.35	9.35	100	100	0.0017	0.556
	30	2	60	0.040	0.0016	9.35	9.35	10	10	0.0073	0.560

* Bed porosity, $\epsilon = 0.40$; Temp. of PSA operation = 298 K; P_L = 1 atm (101.3 kPa); P_H = 3 atm (303.9 kPa); $k_A = 15\,D_A/r^2$; $k_B = 15\,D_B/r^2$.

length to feed inlet velocity ratio, and purge to feed velocity ratio considered in this study, which will reasonably approximate those employed in an industrial-scale operation, there exists a critical time for adsorption. The product purity which, in the present case is the purity of nitrogen, is likely to suffer if the time for steps 1 and 3 is either below or above this critical value.

Increasing the pressure ratio (P_H/P_L) from 2 to 5 did not have any significant effect on the cyclic steady state oxygen exit composition, with the composition being 0.0077 for a pressure ratio of 2 and 0.0081 for a ratio of 5. The effect of axial dispersion which, although not likely to be important in a full-scale unit may well be important in a laboratory-scale unit, was also investigated; the results are included in Tables 1 and 2. With decreasing Peclet number (more backmixing) the nitrogen purity is reduced as expected.

The assumption of frozen solid phase concentration for nitrogen during blowdown for the two sets of simulations (Tables 1 and 2) is reasonable since the diffusivity of nitrogen in carbon sieve is quite low. For oxygen, however, the reality must lie somewhere between the equilibrium and frozen bed assumptions.

Limited performance data for a commercial PSA unit with carbon sieve as the adsorbent have been reported by Knoblauch (1978). Oxygen compositions in the product are in the range of 0.1–1% at an operating pressure of 3 atm (303.9 kPa). This is of the same order as the composition predicted from the present simulation. However, since the process considered by Knoblauch utilizes vacuum desorption rather than blowdown and purge for regeneration, a precise comparison is not possible.

Although based on a somewhat idealized description of the PSA cycle, the present model appears to provide a reasonably good representation of the behavior of the carbon sieve PSA air separation process. Perhaps the most serious approximation lies in the use of linearized rate expressions in place of the full diffusion equations to present the sorption kinetics. It is in principle possible to extend the model to include diffusional rate equations but only at the expense of a considerable increase in the complexity of the numerical calculations.

NOTATION

$A^x_{k,j}$ = collocation coefficient for the gradient, external fluid phase

$A^\tau_{k,j}$ = collocation coefficient for the gradient in the time direction

$B^x_{k,j}$ = collocation coefficient for the Laplacian, external fluid phase

C_{Ai} = adsorbate concentration of component A in fluid phase for bed i, gmol/cm^3

C_{Bi} = adsorbate concentration of component B in fluid phase for bed i, gmol/cm^3

C_{HP} = total concentration of fluid corresponding to pressure P_H, gmol/cm^3

C_{LP} = total concentration of fluid corresponding to pressure P_L, gmol/cm^3

D = micropore diffusivity, cm^2/s

D_A = micropore diffusivity of component A, cm^2/s

D_B = micropore diffusivity of component B, cm^2/s

D_{L1} = axial dispersion coefficient for flow in bed 1 during step 1, cm^2/s

D_{L2} = axial dispersion coefficient for flow in bed 2 during step 1, cm^2/s

G = purge to feed velocity ratio, v_{OL}/v_{OH}

K_A = adsorption equilibrium constant for component A

K_B = adsorption equilibrium constant for component B

k_A = overall mass transfer coefficient for component A, s^{-1}

k_B = overall mass transfer coefficient for component B, s^{-1}

L = length of adsorption bed, cm

Pe_H = Peclet number for high-pressure flow in bed 2 during step 1, Lv_{OH}/D_{L2}

Pe_L = Peclet number for low-pressure flow in bed 1 during step 1, Lv_{OH}/D_{L1}

q_{Ai} = adsorbate concentration of component A in solid phase for bed i, gmol/cm^3

q_{Bi} = adsorbate concentration of component B in solid phase for bed i, gmol/cm^3

q^*_{Ai}, q^*_{Bi} = defined by Eqs. 7 and 16 for $i = 2$ and $i = 1$, respectively, gmol/cm^3

t = time, s

t_{max} = maximum period for which adsorption in bed 2 and desorption in bed 1 are carried out simultaneously during step 1, s; also the maximum period for which adsorption in bed 1 and desorption in bed 2 are carried out simultaneously during step 3

V_1 = v_1/v_{OH}, interstitial fluid velocity in bed 1

V_2 = v_2/v_{OH}, interstitial fluid velocity in bed 2

v_1 = interstitial fluid velocity in bed 1, cm/s

v_2 = interstitial fluid velocity in bed 2, cm/s

v_{OH} = interstitial fluid velocity at the inlet of the bed in which high-pressure flow adsorption is carried out, cm/s

v_{OL} = interstitial flow velocity at the inlet of the bed in which low-pressure flow desorption is carried out, cm/s

X_{Ai} = C_{Ai}/C_{HP} or C_{Ai}/C_{LP} depending on whether high-pressure flow adsorption or low-pressure flow desorption occurs in the ith bed

X_{Bi} = C_{Bi}/C_{HP} or C_{Bi}/C_{LP} depending on whether high-pressure flow adsorption or low-pressure flow desorption occurs in the ith bed; also equal to $(1 - X_{Ai})$

x = dimensionless distance, z/L

Y_{Ai} = $q_{Ai}/K_A C_{HP}$, adsorbate concentration of component A in solid phase in bed i

Y_{Bi} = $q_{Bi}/K_B C_{HP}$, adsorbate concentration of component B in solid phase in bed i

z = axial distance coordinate, cm

Greek Letters

α = ratio of bed length to high pressure feed inlet velocity, L/v_{OH}, s

ϵ = bed porosity

Δ = time increment, s

τ = t/Δ

APPENDIX: SOLUTION BY DOUBLE COLLOCATION

The method of double collocation involves discretizing the spatial as well as the time derivatives in the equations. The resulting nonlinear algebraic equations are then solved using a standard routine.

Assuming the symbol ϕ stands for any one of the variables, X_{A1}, X_{A2}, Y_{A1}, Y_{A2}, Y_{B1}, Y_{B2}, V_1, or V_2, we may write,

$$\left.\frac{\partial \phi}{\partial x}\right|_{ki} = \sum_{j=1}^{M+2} A^x_{kj}\phi_{ji} \tag{A1}$$

$$\left.\frac{\partial^2 \phi}{\partial x^2}\right|_{ki} = \sum_{j=1}^{M+2} B^x_{kj}\phi_{ji} \tag{A2}$$

$$\left.\frac{\partial \phi}{\partial \tau}\right|_{ki} = \sum_{j=1}^{N+2} A^\tau_{ij}\phi_{kj} \tag{A3}$$

The definitions of the various symbols are given in the Notation section.

Given by way of initial conditions are,

$$\begin{aligned} &X_{A2}(k, 1), \quad X_{A1}(k, 1) \quad k = 2 \ldots M+1 \\ &Y_{A2}(k, 1), \quad Y_{A1}(k, 1) \quad k = 1 \ldots M+2 \\ &Y_{B2}(k, 1), \quad Y_{B1}(k, 1) \quad k = 1 \ldots M+2 \\ &V_2(1, i), \quad\quad V_1(1, i) \quad\quad i = 1 \ldots N+2 \end{aligned} \tag{A4}$$

The computation now involves four steps. Note, however, that these steps do not correspond to the four steps of the PSA operation itself.

In step 1, we assume (initial guess) the values of the variables. That is we provide values for,

$$X_{A2}(k, i),\ X_{A1}(k, i) \quad \begin{matrix} k = 2 \ldots M+1 \\ i = 2 \ldots M+1 \end{matrix} \quad \{2M(N+1) \text{ unknowns}\}$$

$$Y_{A2}(k, i),\ Y_{A1}(k, i) \quad \begin{matrix} k = 1 \ldots M+2 \\ i = 2 \ldots N+2 \end{matrix} \quad \{2(M+2)(N+1) \text{ unknowns}\}$$

$$Y_{B2}(k, i),\ Y_{B1}(k, i) \quad \begin{matrix} k = 1 \ldots M+2 \\ i = 2 \ldots N+2 \end{matrix} \quad \{2(M+2)(N+1) \text{ unknowns}\}$$

$$V_2(k, i),\ V_1(k, i) \quad \begin{matrix} k = 2 \ldots M+2 \\ i = 1 \ldots N+2 \end{matrix} \quad \{2(M+1)(N+2) \text{ unknowns}\}$$

Since the number of unknowns is equal to the number of equations, we have in all $\{8(N+1)(M+1)\} + 2(M+N+2)$ equations to solve simultaneously for steps 1 and 3 of the PSA simulation. In the present work, N was 1 and M was 4. A few simulations were, however, performed with $N = 1$, $M = 6$, and $N = 2$, $M = 4$ to confirm the accuracy of the solution.

Step 2 of the computation involves the evaluation of $X_{A2}(1,i)$, $X_{A2}(M+2, i)$. These values can be extracted based on the values of $X_{A2}(k, i)$ and $X_{A1}(k, i)$ for $K = 2 \ldots M+1$ and $i = 2 \ldots N+2$, from the dimensionless form of the boundary conditions given by Eqs. 8, 9, 17, and 19, which, when written in collocation form would be, for high-pressure flow in bed 2 during step 1,

$$\sum_{j=1}^{M+2} A^x(1, j)X_{A2}(j, i) = -Pe_H[X_{A2}|_{x=0^-} - X_{A2}(1, i)] \tag{A5}$$

$$\sum_{j=1}^{M+2} A^x(M+2, j)X_{A2}(j, i) = 0 \tag{A6}$$

and for low-pressure flow in bed 1,

$$\sum_{j=1}^{M+2} A^x(1, j)X_{A1}(j, i) = -GPe_L[X_{A1}|_{x=0^-} - X_{A1}(1, i)] \tag{A7}$$

$$\sum_{j=1}^{M+2} A^x(M_2, j)X_{A1}(j, i) = 0 \tag{A8}$$

In step 3, knowing now the values of the variables at all points in the two beds, we compute

$$\left.\frac{\partial \phi}{\partial x}\right|_{k,i}, \quad \left.\frac{\partial^2 \phi}{\partial x^2}\right|_{k,i}, \quad \text{and} \quad \left.\frac{\partial \phi}{\partial \tau}\right|_{k,i}$$

Step 4 involves setting up the residuals $R^\phi_{k,i}$ and updating the initial guess to force the $\{8(N+1)(M+1)\} + 2(M+N+2)$ residuals to become zero. For example, for X_{A2}, Y_{A2}, Y_{B2}, and V_2 during high-pressure flow adsorption in bed 2 (step 1) we write,

$$\begin{aligned} R^{X_{A2}}_{k,i} = &\alpha \sum_{j=1}^{N+2} A^\tau_{i,j} \cdot X_{A2}(k, j) - \frac{1}{Pe_H} \cdot \Delta \cdot \sum_{j=1}^{M+2} B^x_{k,j} \cdot X_{A2}(j, i) \\ &+ V_2(k, i) \cdot \Delta \cdot \sum_{j=1}^{M+2} A^x_{k,j} \cdot X_{A2}(j, i) \\ &+ \left\{\left(\frac{1-\epsilon}{\epsilon}\right) \cdot \alpha \cdot \Delta \cdot k_A \cdot K_A \cdot [X_{A2}(k, i) \right. \\ &\left. - Y_{A2}(k, i)] \cdot (1.0 - X_{A2}(k, i))\right\} \\ &- \left\{\left(\frac{1-\epsilon}{\epsilon}\right) \cdot \alpha \cdot \Delta \cdot k_B \cdot X_{A2}(k, i) \right. \\ &\left. \cdot K_B \cdot [(1.0 - X_{A2}(k, i)) - Y_{B2}(k, i)]\right\} = 0 \end{aligned} \tag{A9}$$

where $k = 2 \ldots M+1$; $i = 2 \ldots N+2$

$$R_{k,i}^{Y_{A2}} = \sum_{j=1}^{N+2} A_{i,j}^{T} \cdot Y_{A2}(k, j) - k_A \cdot \Delta \cdot [X_{A2}(k, i) - Y_{A2}(k, i)] = 0 \tag{A10}$$

where $k = 1 \ldots M + 2, i = 2 \ldots N + 2$

$$R_{k,i}^{Y_{B2}} = \sum_{j=1}^{N+2} A_{i,j}^{T} \cdot Y_{B2}(k, j) - k_B \cdot \Delta \cdot [(1.0 - X_{A2}(k, i)) - Y_{B2}(k, i)] = 0 \tag{A11}$$

where $k = 1 \ldots M + 2, i = 2 \ldots N + 2$

$$R_{k,i}^{V_2} = \sum_{j=1}^{M+2} A_{k,j}^{x} \cdot V_2(j, i) + \left\{\left(\frac{1-\epsilon}{\epsilon}\right) \cdot \alpha \cdot k_A \cdot K_A \cdot [X_{A2}(k, i) - Y_{A2}(k, i)]\right\} + \left\{\left(\frac{1-\epsilon}{\epsilon}\right) \cdot \alpha \cdot k_B \cdot K_B \cdot [(1.0 - X_{A2}(k, i)) - Y_{B2}(k, i)]\right\} = 0 \tag{A12}$$

where $k = 2 \ldots M + 2; i = 2 \ldots N + 2$.

Similarly, equations for X_{A1}, Y_{A1}, Y_{B1} and V_1 are written for the low-pressure purge flow in bed 1 (step 1).

The algorithm ZSPOW as given in the IMSL package is used to solve the nonlinear algebraic equations to get the distribution of X_{A2}, X_{A1}, Y_{A2}, Y_{A1}, Y_{B2}, Y_{B1}, V_2, and V_1 in the two beds at $\tau = 1$ or $t = \Delta$. The procedure is repeated until $t = t_{max}$ = duration of time for the first step (adsorption) in bed 2 and desorption (purging) in bed 1.

After the approximations for step 2 of the PSA, the nonlinear algebraic equations for step 3 [adsorption in bed 1 and desorption (purging) in bed 2] are solved, which is followed by the approximations for step 4. This essentially completes the computations for one cycle of the PSA operation. The computations for the next cycle involve the solution for the nonlinear algebraic equations for step 1 with the initial conditions based on the profile in the beds at the end of the previous cycle. The computations continue until cyclic steady state is reached, when there is no further change in the composition profiles in the beds between two successive cycles. The number of cycles required to reach the steady state in the simulations reported here was typically 12.

LITERATURE CITED

Chan, Y. N., F. B. Hill, and Y. W. Wong, "Equilibrium Theory of a Pressure Swing Adsorption Process," *Chem. Eng. Sci.*, **36**, 243 (1981).

Chihara, K., and M. Suzuki, "Simulation of Nonisothermal Pressure Swing Adsorption," *J. Chem. Eng. Japan*, **16**(1), 53 (1983).

Flores-Fernandez, G., and C. N. Kenney, "Modeling of the Pressure Swing Air Separation Process," *Chem. Eng. Sci.*, **38**, 827 (1983).

Knaebel, K. S., and F. B. Hill, "Analysis of Gas Purification by Heatless Adsorption," Paper No. 91d, AIChE Ann. Meet., Los Angeles (Nov., 1982).

Knoblauch, K., "Pressure Swing Adsorption Geared for Small Volume Users," *Chem. Eng.*, **87**, (Nov., 1978).

Mitchell, J. E., and L. H. Shendalman, "Study of Heatless Adsorption in the Model System CO_2 in He. II," *AIChE Symp. Ser.*, **69**(134), 25 (1973).

Raghavan, N. S., M. M. Hassan, and D. M. Ruthven, "Numerical Simulation of a PSA System. I: Isothermal Trace Component System with Linear Equilibrium and Finite Mass Transfer Resistance," *AIChE J.*, **31**, 385 (1985).

Shendalman, L. H., and J. E. Mitchell, "A Study of Heatless Adsorption in the Model System CO_2 in He. I," *Chem. Eng. Sci.*, **27**, 1,449 (1972).

Turnock, P. H., and R. H. Kadlec, "Separation of N_2 and CH_4 via Periodic Adsorption," *AIChE J.*, **17**, 335 (1971).

Young, L. C., and B. A. Finlayson, "Axial Dispersion in Nonisothermal Packed Bed Chemical Reactors," *Ind. Eng. Chem. Fund.*, **12**(4), 412 (1973).

Manuscript received July 25, 1984, and revision received Feb. 4, 1985.